ORGANOMETALLICS

Article

pubs.acs.org/Organometallics

Ruthenium PNN(O) Complexes: Cooperative Reactivity and Application as Catalysts for Acceptorless Dehydrogenative Coupling Reactions

Sandra Y. de Boer, Ties J. Korstanje, Stefan R. La Rooij, Rogier Kox, Joost N. H. Reek, and Jarl Ivar van der Vlugt*

Homogeneous, Supramolecular & Bio-inspired Catalysis, van 't Hoff Institute for Molecular Sciences, University of Amsterdam, Science Park 904, 1098 XH Amsterdam, The Netherlands

Supporting Information

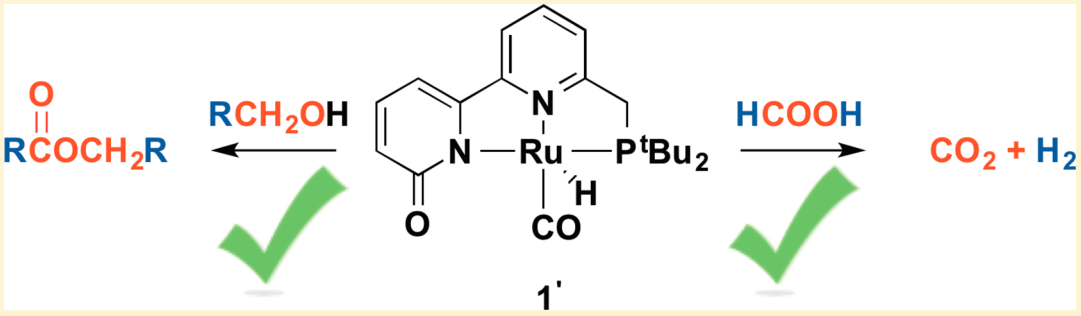

ABSTRACT: The novel tridentate PNN^{OH} pincer ligand $\mathbf{L}^{H}$ features a reactive 2-hydroxypyridine functionality as well as a bipyridyl-methylphosphine skeleton for meridional coordination. This proton-responsive ligand coordinates in a straightforward manner to RuCl(CO)(H)(PPh_3)$_3$ to generate complex **1**. The methoxy-protected analogue $\mathbf{L}^{Me}$ was also coordinated to Ru(II) for comparison. Both species have been crystallographically characterized. Site-selective deprotonation of the 2-hydroxypyridine functionality to give **1′** was achieved using both mild (DBU) and strong bases (KO^{t}Bu and KHMDS), with no sign of involvement of the phosphinomethyl side arm that was previously established as the reactive fragment. Complex **1′** is catalytically active in the dehydrogenation of formic acid to generate CO-free hydrogen in three consecutive runs as well as for the dehydrogenative coupling of alcohols, giving high conversions to different esters and outperforming structurally related PNN ligands lacking the N^{OH} fragment. DFT calculations suggest more favorable release of H_2 through reversible reactivity of the hydroxypyridine functionality relative to the phosphinomethyl side arm.

INTRODUCTION

Reactive ligand design has opened up fundamentally novel pathways for bond activation, small-molecule functionalization, and homogeneous catalysis. Tridentate pincer ligands that feature a reactive site have gained a great deal of interest during the past decade.[1−3] Among several design types, lutidine-based PNP systems (Figure 1a) and analogues thereof have particularly gained momentum as ligands of choice for a range of transformations, because of their ability to undergo facile and reversible deprotonation of the phosphinomethyl side arm, generating a formally dearomatized N-heterocycle.[4] Recently, also bis(pyrazole)-appended pyridines (Figure 1b)[5] and pyridone-containing (^{OH}NNN^{OH}) derivatives[6] (Figure 1c) have attracted much attention as pH-responsive pincer frameworks in the context of metal−ligand bifunctional catalysis.

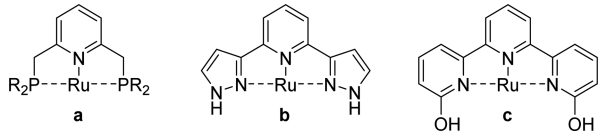

Figure 1. Reactive ligand designs based on symmetric pincer frameworks with two identical reactive sites.

All three systems can be qualified as outer-sphere reactive ligands, as the proton-responsive (C−H, N−H, or O−H) functionality is not located directly in the first coordination sphere of the metal center. This sets these systems apart from ligands that demonstrate reversible amino/amido[7,8] or reversible cyclometalation reactivity.[9] However, the overall geometric features as well as the steric and electronic characteristics of e.g. PN vs. N^{OH} frameworks are different, with respect to both acidity, orientation, and location of the protic hydrogen relative to the metal center geometry and distance to bound substrate or hydride fragments on the metal. Next to the design of symmetric reactive pincer ligands, nonsymmetric tridentate systems that incorporate ligand

Received: February 13, 2017
Published: April 6, 2017

DOI: 10.1021/acs.organomet.7b00111
Organometallics 2017, 36, 1541−1549

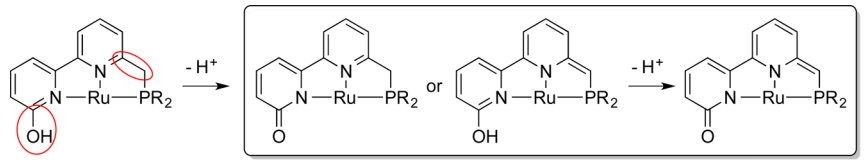

Figure 2. Envisioned design of a PNN^{OH} system with two different types of proton-responsive sites.

Scheme 1. Synthetic Route for the Preparation of Ligand L^H and Ru(II) Complexes 1 and 1_{MeCN}

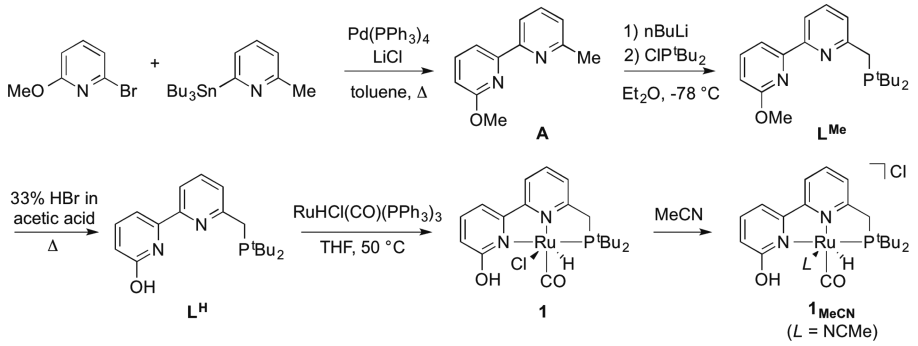

reactivity have shown potential application in cascade catalysis.[10,11] There is currently no system that combines both PN *and* N^{OH} reactive ligand-based functionalities or studies that compare both functionalities with respect to activation and catalytic performance.

Ruthenium complexes bearing reactive pincer ligands have demonstrated catalytic competence in a substantial variety of reactions, including acceptorless dehydrogenation of alcohols into ketones, the hydrogenation of amides into alcohols and amines, and the reverse reaction: i.e., amide formation from alcohols and amines.[12] In these catalytic reactions metal−ligand cooperativity is crucial, as reversible deprotonation of the phosphinomethyl arm is required during the catalytic cycle. In order to address the catalytic competence of a rigid pincer unit incorporating both the well-established PN coordination mode *and* the reactive N^{OH} fragment, and related to ongoing studies in our group on the application of reactive ligands for substrate activation and catalysis,[13] we herein introduce the new ligand L^H based on 6-(di-*tert*-butylphosphinomethyl)-6′-hydroxy-2,2′-bipyridine (Figure 2). Coordination of this ligand to Ru(Cl)(CO)(H)$(PPh_3)_3$ has enabled stoichiometric reactivity studies with various bases and Ru-catalyzed dehydrogenative (coupling) reactions. We show the added value of this skeleton relative to other reactive PNN scaffolds for these reactions.

RESULTS AND DISCUSSION

Synthesis of Tridentate PNN(O) Ligand L^H and Coordination to Ru(II). The synthesis of ligand L^H was straightforward, despite the multistep approach, and comparable to the synthesis of bipyridine PNN ligands.[4d] Intermediate **A** was synthesized according to a literature procedure[14] via a Stille coupling using 2-bromo-6-methoxypyridine and 2-methyl-6-(tributylstannyl)pyridine (Scheme 1). Monolithiation of the methyl group and subsequent phosphorylation with ClP^tBu_2 yielded L^{Me}. In the last step, removal of the methoxy group was not successful using BBr_3, but acid hydrolysis using concentrated HBr in acetic acid produced ligand L^H in 69% yield.

^{31}P NMR spectroscopy of ligand L^H results in a singlet at δ 37.5, while the ^1H NMR spectrum displays a broad singlet at 11.97 ppm and a doublet ($^2J_{PH}$ = 3.2 Hz) at 3.16 ppm, which correspond to the hydroxyl proton and $-CH_2P$ spacer, respectively. These spectral data are very similar to those of the bipyridine-based PNN ligand,[4d] suggesting negligible electronic influence of the hydroxyl group. The elemental composition of the species was furthermore confirmed by HR-MS analysis. Reaction of L^H with RuCl(CO)(H)$(PPh_3)_3$ yielded an orange solid that was fully characterized and identified as RuCl(CO)(H)(L^H), complex **1** (Scheme 1). The ^{31}P NMR spectrum displays a singlet at 104.4 ppm, and in the ^1H NMR spectrum the hydride is found as a broad doublet at δ −19.32 ($^2J_{PH}$ = 23.8 Hz). Furthermore, the corresponding IR spectrum shows a strong band at 1916 cm^{-1} for the CO ligand and the HR-MS analysis (m/z 461.0937 [M − Cl]; calcd 461.0936 [M − Cl]) is in agreement with the proposed structure.

Single crystals of complex **1**, grown by slow diffusion of diethyl ether into a concentrated acetonitrile solution, proved suitable for X-ray structure determination (Figure 3). The molecular structure of **1** reveals a distorted-octahedral geometry around the ruthenium center, with the CO ligand trans to the central pyridine of the PNN system. The ligand is not completely planar, as the methylene $-CH_2$ group shows the expected out-of-plane bending. The chloride ligand acts as a noncoordinating counterion, with an acetonitrile fragment coordinated to Ru to provide $\mathbf{1}_{MeCN}$. A hydrogen-bonding interaction is observed between the hydroxyl moiety and the noncoordinating chloride atom. The asymmetric unit cell contains both enantiomers as a racemate. We also performed the coordination of the methoxy ether protected ligand precursors L^{Me} with RuCl(CO)(H)$(PPh_3)_3$, which resulted in the formation and crystallization of complex RuCl(CO)(H)(L^{Me}), $\mathbf{1}^{Me}$ (see the Supporting Information for details), with PNN coordination and structural features very comparable to those found for **1**.

Ligand-Based Reactivity of Complex 1. We hypothesized that the 2-hydroxypyridine moiety of the ligand would be susceptible to preferential deprotonation over the methylene bridgehead and by bases weaker than those typically used for the deprotonation of lutidine-derived pincer frameworks (such

DOI: 10.1021/acs.organomet.7b00111
Organometallics 2017, 36, 1541−1549

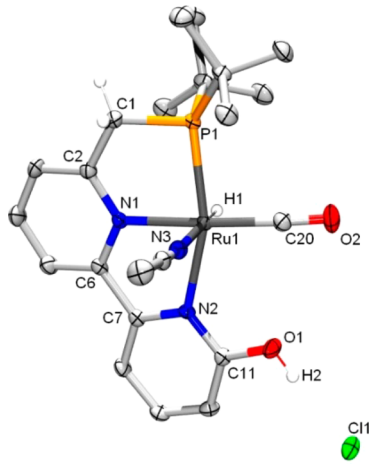

Figure 3. ORTEP plot (50% probability displacement ellipsoids) of the complex $\mathbf{1}_{MeCN}$, [Ru(CO)(H)(NCMe)($\mathbf{L}^{H}$)]Cl. Hydrogen atoms have been omitted for clarity, except for those on C1, O1, and Ru1. Selected bond lengths (Å), angles, and torsion angles (deg), for **1**: Ru1−P1 2.2711(6); Ru1−N1 2.0964(19); Ru1−N2 2.1598(18); Ru1−C20 1.8524(25); Ru1−H1 1.71(3); Ru1−N3 2.1855(21); C20−O2 1.1512(30); H2- - -Cl1 2.153; P1−Ru1−N1 82.72(5); P1−Ru1−N2 157.27(7); N1−Ru1−N2 76.24(7); N1−Ru1−C20 171.49(9); H1−Ru1−N3 171.90(1.04); N2−C7−C6−N1 −1.00; N1−C2−C1−P1 29.04.

as KO^{t}Bu or KHMDS). Addition of 1 equiv of NEt_3 (pK_a value in DMSO: 9)[15] to complex **1** did not lead to proton transfer, according to ^{1}H NMR spectroscopy, but reaction with DBU (1,8-diazabicyclo[5.4.0]undec-7-ene) (pK_a value in DMSO: 12) gave an immediate color change from orange to brown-red, providing selective deprotonation of the 2-hydroxypyridine unit to generate complex **1′** (Scheme 2). Using 1 equiv of KO^{t}Bu or KHMDS at −32 °C also led to **1′**, indicating that the 2-hydroxypyridine is the ultimate site for deprotonation.[16] Addition of acid to a solution of **1′** regenerates **1**.

Scheme 2. Deprotonation of complex 1 (weak and strong base) to afford 1′

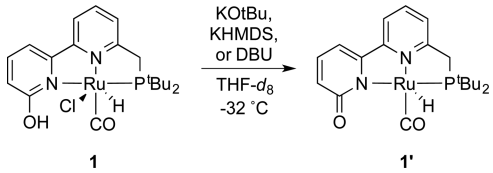

The transformation of **1** into **1′** coincides with only a small shift in the ^{31}P NMR spectrum to 102.7 ppm ($\Delta\delta$ = 1.7 ppm), suggesting that the overall donor capabilities of the pyridone unit are fairly similar to that of the parent 2-hydroxypyridine unit. In the ^{1}H NMR spectrum a doublet is observed at δ −19.47 (J_{PH} = 25 Hz) for the hydride and an ABX system centered around 3.80 and 3.63 ppm supports an intact methylene spacer.

Catalytic Activity of 1 in the Dehydrogenation of HCOOH. Hydrogen is potentially one of the major energy carriers for the future, and formic acid has been demonstrated to provide an interesting storage-release system for the reversible storage of dihydrogen.[17] Formic acid dehydrogenation is typically performed using (sub)stoichiometric equivalents of base, but this negatively affects the hydrogen content of this storage material. Thus, catalytic dehydrogenation ideally would not require base or other additives. Ruthenium complexes bearing other types of pH-responsive ligands have been shown to be efficient catalysts for the reversible hydrogenation of CO_2 to formic acid.[18] Complex **1′** was found to be a competent catalyst for the base-free dehydrogenation of HCOOH (Scheme 3).[19,20] When only 1 equiv of formic acid was added to complex **1′**, generated in situ from **1** and KO^{t}Bu, a slight color change was observed from brown-red to orange-red, concomitant with the evolution of small bubbles of gas from the solution and detection of species **1′** in the ^{31}P NMR spectrum. We postulate the intermediacy of dihydride species $\mathbf{1}^{HH}$, generated by proton and hydride transfer from formic acid to **1′**.

Next, a catalytic experiment was performed using 10 mol% of **1′**, generated in situ from **1** and base, in dioxane as solvent at 75 °C. The dehydrogenation of formic acid was monitored volumetrically for three consecutive catalytic runs (Figure 4).

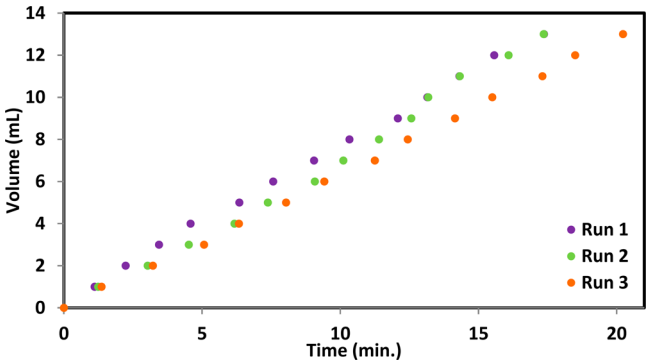

Figure 4. Volumetric response to formic acid dehydrogenation with 10 mol% of complex **1′**, measured in volume of produced gas (H_2 + CO_2) for three consecutive reactions.

The three linear curves have very similar slopes, leading to turnover frequencies of 35, 33, and 29 h^{-1}, indicating that the catalyst is robust and does not decompose upon reuse. Only H_2 and CO_2 were detected by GC, with no trace of CO (detection limit 10 ppm), meaning that clean dihydrogen is formed under these conditions.

On the basis of these data and literature reports on related base-free systems for formic acid dehydrogenation,[19,20] the following mechanism is proposed for the cooperative

Scheme 3. Complex 1′ in the Stoichiometric Dehydrogenation of HCOOH

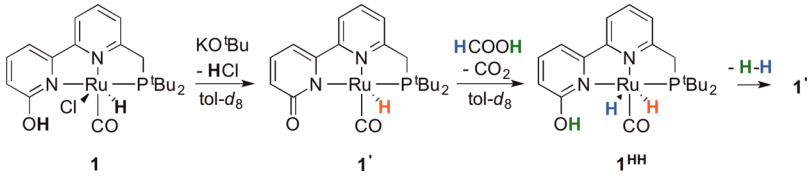

DOI: 10.1021/acs.organomet.7b00111
Organometallics 2017, 36, 1541−1549

Scheme 4. Proposed Mechanism for the Cooperative Dehydrogenation of Formic Acid with Complex 1′

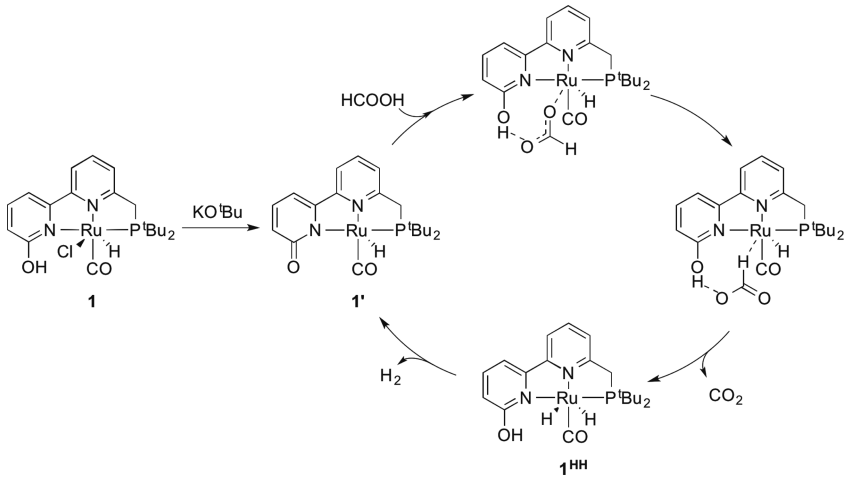

dehydrogenation of formic acid with complex **1′** (Scheme 4). Initially, HCOOH coordinates to deprotonated species **1′**. The protic hydrogen of formic acid binds via a hydrogen bond to the ligand pyridonato group, which induces activation of the O−H bond, while the C═O fragment coordinates to the Ru center via the neutral oxygen. As there is likely no available vacant site on the metal (dissociation of a reprotonated pyridone group by Ru−N bond breaking is unlikely but cannot be ruled out on the basis of these data), *β*-H elimination is deemed not preferred. Therefore, a rearrangement is necessary that involves a rotation around the O−H bond to generate a species in which the formate hydrogen (*H*COO$^-$) atom coordinates to the ruthenium, concomitant with proton transfer to the pyridonato oxygen. This direct hydride transfer or ligand-assisted direct hydride transfer generates the release of carbon dioxide, which is accompanied by the formation of complex $\mathbf{1}^{HH}$. In the final step the deprotonated species **1′** is regenerated, concomitant with the release of H_2.

Catalytic Activity of 1′ in the Acceptorless Dehydrogenative Coupling of Alcohols. Ruthenium pincer complexes have previously been successfully applied in the bifunctional activation of O−H bonds, a feature that can subsequently be used in dehydrogenative coupling reactions: e.g., to generate esters from alcohols with release of H_2.[21] We were interested in probing the catalytic competence of the reactive ligand scaffold in **1** and to find out how this system compares with known Ru(PNN) systems in the acceptorless catalytic dehydrogenative coupling of alcohols to esters, given the different geometric and electronic features of the reactive pyridone C═O. Having established the O−H bond activation of BzOH, this substrate was subjected to literature conditions to afford 90% conversion to benzyl benzoate in 15 h without any formation of the aldehyde (based on GC and NMR analysis), thereby outperforming a RuH(CO)(Cl)(PNN) complex bearing a 2-(diethylaminomethyl)-6-(di-*tert*-butylphosphinomethyl)pyridine PNN ligand (95% conversion in 24 h).[22] Complex $\mathbf{1}^{Me}$ shows only 52% conversion to benzyl benzoate after 16 h, indicating the positive effect of the availability of the pyridone C═O unit on the catalysis. The derivative $\mathbf{1}_{MeCN}$ is inactive under these conditions, likely due to strong binding of acetonitrile, preventing substrate coordination, while complex **1** is also active at 70 °C (74% conversion in 28 h), but no conversion is observed at room temperature. In the presence of DBU as external base, surprisingly, no turnover was obtained after 20 h at 117 °C. Although the deprotonation of complex **1** occurred smoothly with DBU in THF, the lack of activity could be caused by the reduced base strength of DBU in toluene due to the lower polarity of the medium.[23] We also studied the dehydrogenative coupling of 1-butanol to generate butyl butyrate. Catalyst **1** (1 mol %) gave full conversion to the desired product after 15 h at 117 °C with 1 mol % of KOtBu in toluene, thus outperforming the reaction with benzyl alcohol. The benchmark RuH(Cl)(CO)(PNN) complex again requires 72 h to achieve 92% conversion.

On the basis of the above data and the well-known reactivity of the PNP and PNN pincer complexes with a reactive methylene spacer in the ligand backbone, we propose a plausible catalytic cycle for the dehydrogenative coupling of alcohols by preactivated complex **1′**, involving the hydroxypyridine functionality (Scheme 5). Initially, activation of the alcohol O−H bond results in ligand side arm rearomatization, to form alkoxide complex **2**. In the following step $\mathbf{1}^{HH}$ is formed, presumably via dissociation of the reprotonated pyridone group by Ru−N bond breaking, concomitant with

Scheme 5. Proposed Catalytic Cycle for the Dehydrogenative Coupling of Alcohols to Esters Using Complex 1 as Precatalyst and Involving 1′ in the Cycle

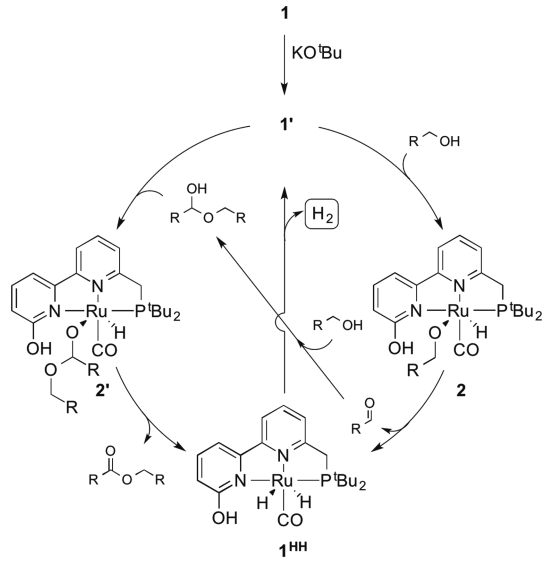

DOI: 10.1021/acs.organomet.7b00111
Organometallics 2017, 36, 1541−1549

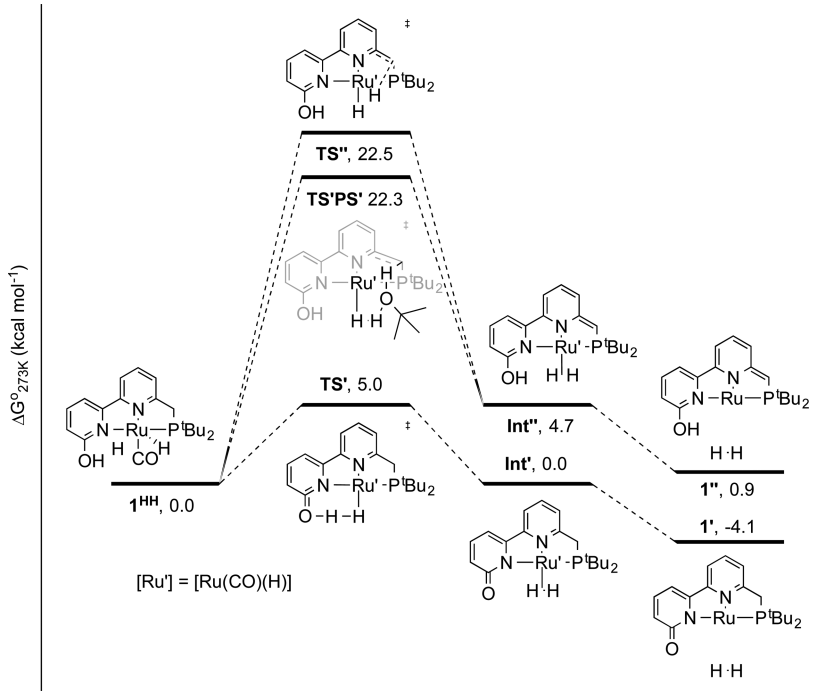

Figure 5. Potential energy diagram (DFT, BP86, def2-TZVP, disp3) for the formation of **1′**, **1″**, and dihydrogen from $\mathbf{1}^{HH}$; $\Delta G^{\circ}_{273\,K}$ values are given in kcal mol^{-1}, with complex $\mathbf{1}^{HH}$ taken as a reference point. One hydride ligand and the CO ligand were omitted for clarity in the depiction of **TS′**, **TS″**, **TS′PS′**, **Int′**, and **Int″**.

formation of the aldehyde. Elimination of dihydrogen then regenerates complex **1′**. The aldehyde condenses with alcohol directly or condenses in a metal-catalyzed fashion[24] to form the hemiacetal, which (upon reaction with complex **1′**) leads to aromatized complex **2′**. Dehydrogenation via *β*-H elimination eliminates the ester and generates *trans*-dihydride complex $\mathbf{1}^{HH}$, from which another equiv of dihydrogen is then liberated to regenerate complex **1′**, completing the catalytic cycle. Alternatively, inner-sphere formation of the hemiacetal by coupling of the bound alkoxide with alcohol from solution may proceed as well.

Computational Investigations into Dihydrogen formation. As can be seen in the above proposed catalytic cycles, the central complex formed is $\mathbf{1}^{HH}$, concomitant with the release of CO_2 (formic acid dehydrogenation) or aldehyde/ester (dehydrogenative coupling of alcohols). To date, no direct comparison has been made between the reactive 2-hydroxypyridine and phosphinomethyl-based functionalities with respect to H_2 release via dehydrogenative pathways. Hence, we decided to perform DFT calculations (BP86, def2-TZVP, disp3), and the obtained energy profiles are displayed in Figure 5. The aromatized *trans*-dihydride complex $\mathbf{1}^{HH}$ was used as a reference point (0.0 kcal mol^{-1}). Starting from this complex, transition state **TS′** (H_2 formation over the pyridone) is 5.0 kcal mol^{-1} higher in free energy, while the barrier for **TS″** (H_2 formation over the phosphinomethyl) is 22.5 kcal mol^{-1}. However, proton shuttling via ^{t}BuOH, obtained from protonation of KO^{t}Bu, could be involved, which could lower the barrier significantly.[9b,25] Remarkably, the barrier of **TS′PS′** is lowered only marginally and is thus still much higher (17.3 kcal mol^{-1}) in energy than **TS′**. Subsequent formation of intermediate **Int′** is thermoneutral in comparison to $\mathbf{1}^{HH}$, whereas species **Int″** is slightly uphill in energy by 4.7 kcal mol^{-1}. Liberation of dihydrogen is found to be exergonic by roughly 4 kcal mol^{-1} for both complexes. Overall, the formation of dihydrogen is exergonic by −4.1 kcal mol^{-1} for **1′** and slightly endergonic by 0.9 kcal mol^{-1} for **1″**, demonstrating that the pathway is both kinetically and thermodynamically favored via the hydroxy-pyridine species.

CONCLUSIONS

The novel rigid dual-mode reactive PNN^{OH} pincer ligand $\mathbf{L}^{H}$ bearing two different cooperative sites is easily synthesized, and coordination to ruthenium allows access to Ru(Cl)(CO)(H)-($\mathbf{L}^{H}$) complex **1**, which was crystallographically characterized as the MeCN adduct. Reaction of complex **1** with DBU leads to selective deprotonation of the hydroxypyridine functionality, providing activated complex **1′**. An excess of this weak base did not induce dearomatization via deprotonation of the phosphinomethyl side arm functionality. Application of complex **1** in the dehydrogenation of formic acid produces CO-free dihydrogen with a turnover frequency of 30 h^{-1} for several consecutive runs, demonstrating catalyst robustness. Despite the ease of deprotonation of **1** relative to other complexes bearing proton-responsive ligands, only moderate catalytic activity in formic acid dehydrogenation was obtained under these unoptimized conditions. Complex **1** is also catalytically active in the dehydrogenative coupling of alcohols into esters, resulting in 90% conversion for benzyl alcohol and full conversion for 1-butanol. As such, this system outperforms related Ru(PNN) species, illustrating the beneficial role of the 2-hydroxypyridine reactive side arm. DFT calculations suggest an active role for the pyridone side arm in H_2 liberation in these catalytic conversions.

EXPERIMENTAL SECTION

General Procedures. Solvents were either distilled over suitable drying agents or dried using an MBraun SPS (Solvent Purification System). All experiments were carried out under an inert-gas atmosphere using standard Schlenk techniques. All chemicals were

DOI: 10.1021/acs.organomet.7b00111
Organometallics 2017, 36, 1541−1549

commercially available and used without further purification, unless described otherwise. The ^{1}H, $^{1}H\{^{31}P\}$, $^{31}P\{^{1}H\}$, and $^{13}C\{^{1}H\}$ NMR spectra were recorded at room temperature on Bruker AV400 (at 400, 162, and 100 MHz, respectively) and Bruker DRX500 instruments (at 500, 202, and 126 MHz, respectively) and calibrated to the residual proton and carbon signals of the solvent[26] or to 85% H_3PO_4 externally. High-resolution mass spectra were recorded on a JEOL AccuTOF GC v 4g, JMS-T100GCV mass spectrometer (FD) and on a JEOL AccuTOF LC, JMS-T100LP mass spectrometer (CSI). IR spectra were recorded with a Bruker Alpha-p FT-IR spectrometer operated in the ATR mode. GC analysis for esters and amides was performed on a Thermo Scientific Trace GC Ultra equipped with a Restek RTX-200 column (30 m × 0.25 mm × 0.5 μm). Temperature program: initial temperature 50 °C, hold for 4 min, heat to 130 °C with 30 °C/min, hold for 2 min, heat to 250 °C with 50 °C/min, hold for 9 min. Other conditions: inlet temperature 200 °C, split ratio of 60, 1 mL/min carrier flow, FID temperature 250 °C.

Syntheses and Characterization. *2-Methyl-6-(tributylstannyl)-pyridine.* This synthesis was based on a literature procedure.[27] 2-Bromo-6-methylpyridine (7.56 g, 43.9 mmol) was dissolved in THF (20 mL) and cooled to −78 °C. A 2.5 M solution of *n*-BuLi in hexanes (17.6 mL, 43.9 mmol) was added over the course of 20 min and the mixture was stirred for 3 h more at −78 °C. Tributyltin chloride (14.3 g, 43.9 mmol) was added, and the mixture was allowed to warmed to room temperature overnight. The reaction was quenched with saturated NH_4Cl solution (40 mL) and extracted with ethyl acetate (3 × 100 mL). The combined organic layers were washed with water and brine (both 50 mL), dried over Na_2SO_4, and concentrated in vacuo to give a yellow oil (16.58 g, quantitative). ^{1}H NMR (300 MHz, chloroform-*d*, ppm): δ 7.39 (t, J_H = 7.5 Hz, 1H, py*H*), 7.20 (d, J_{HH} = 7.5 Hz, 1H, py*H*), 6.98 (dd, J_{HH} = 7.9, 1.1 Hz, 1H, py*H*), 2.57 (s, 3H, CH_3), 1.64−1.54 (m, 6H, SnBu), 1.36 (h, J_{HH} = 7.2 Hz, 6H, SnBu), 1.18−1.07 (m, 6H, SnBu), 0.91 (t, J_{HH} = 7.3 Hz, 9H, SnBu). ^{13}C NMR (75 MHz, chloroform-*d*, ppm): δ 173.04 (s, pyC), 158.57 (s, pyC), 133.23 (s, pyCH), 129.33 (s, pyCH), 121.45 (s, pyCH), 29.13 (s, CH_2), 27.37 (s, CH_2), 24.93 (s, CH_3), 13.72 (s, CH_3), 9.85 (s, CH_2). HRMS (FD+) ($C_{18}H_{33}NSn$): *m*/*z* calcd, 383.16380 $[M]^+$; found, 383.17925 $[M]^+$.

Compound A, 6-Methoxy-6′-methyl-2,2′-bipyridine. This synthesis was based on a literature procedure.[27] 2-Methoxy-6-bromopyridine (8.2 g, 43.4 mmol), $Pd(PPh_3)_4$ (0.5 g, 0.434 mmol), LiCl (3.8 g, 96.8 mmol), and 2-methyl-6-(tributylstannyl)pyridine (16.58 g, 43.4 mmol) were dissolved in toluene (50 mL) and stirred at reflux overnight. The solution was cooled to room temperature, and the organic layer was extracted three times with a 6 M HCl solution (3 × 50 mL). The combined aqueous layers were neutralized with a saturated solution of NH_4OH and then extracted with DCM (3 × 75 mL). The organic layer was washed with water and brine (both 50 mL), dried over Na_2SO_4, and finally concentrated in vacuo to yield a yellow oil (8.68 g, quantitative). ^{1}H NMR (300 MHz, chloroform-*d*, ppm): δ 8.22 (d, J_H = 7.9 Hz, 1H, py*H*), 8.06 (dd, J_H = 7.4, 0.8 Hz, 1H, py*H*), 7.71 (td, J_H = 7.9, 1.8 Hz, 1H, py*H*), 7.23−7.14 (m, 2H, py*H*), 6.78 (dd, J_H = 8.2, 0.8 Hz, 1H, py*H*), 4.07 (s, 3H, OCH_3), 2.65 (s, 3H, Me). ^{13}C NMR (75 MHz, chloroform-*d*, ppm): δ 163.41 (s, pyC), 157.56 (s, pyC), 155.36 (s, pyC), 153.73 (s, pyC), 139.14 (s, pyCH), 136.71 (s, pyCH), 122.94 (s, pyCH), 117.84 (s, pyCH), 113.66 (s, pyCH), 110.80 (s, pyCH), 52.95 (s, OCH_3), 24.54 (s, CH_3). HRMS (FD+) ($C_{12}H_{12}N_2O$): *m*/*z* calcd, 200.09496 $[M]^+$; found, 200.09396 $[M]^+$.

Ligand L^{Me}. 6-Methoxy-6′-methyl-2,2′-bipyridine (1 g, 4.99 mmol) was dissolved in diethyl ether (20 mL) and then cooled to −78 °C. *n*-BuLi (2.5 M solution in hexanes) (2 mL, 5.01 mmol) was added over the course of 20 min, and the reaction mixture was stirred for an additional 1 h at −78 °C. ClP^tBu_2 (0.902 g, 5 m mol) was added and the reaction mixture was warmed to room temperature overnight. The mixture was stirred for an additional 6 days, and the progress of the reaction was checked by ^{31}P NMR every day. Degassed water (20 mL) was added, and the organic layer was separated. The aqueous layer was extracted three more times with diethyl ether (3 × 20 mL), and the combined organic fractions were dried over Na_2SO_4. The solvent was evaporated in vacuo and recrystallized from MeOH to yield off-white crystals. ^{1}H NMR (500 MHz, acetone-d_6, ppm): δ 8.21 (d, J_{HH} = 7.8 Hz, 1H, pyH^3), 8.09 (d, J_{HH} = 7.4 Hz, 1H, py$H^{3'}$), 7.79 (q, J_{HH} = 7.8 Hz, 2H, pyH^4 and py$H^{4'}$), 7.42 (d, J_H = 7.7 Hz, 1H, pyH^5), 6.80 (d, J_{HH} = 8.2 Hz, 1H, py$H^{5'}$), 4.01 (s, 3H, OCH_3), 3.15 (d, J_{PH} = 2.9 Hz, 2H, CH_2). 1.18 (d, J_{PH} = 10.6 Hz, 18H, $P(C(CH_3)_3)_2$). ^{13}C NMR (126 MHz, acetone-d_6, ppm): δ 164.4 (s, pyC$^{6'}$), 162.6 (d, J_{PC} = 14.6 Hz, pyC^6), 155.5 (s, pyC$^{2'}$), 154.7 (s, pyC^2), 140.4 (s, pyC$^{4'}$H), 137.6 (s, 1C, pyC^{4}H), 124.7 (d, J_{PC} = 7.8 Hz, pyC^{5}H), 118.2 (d, J_{PC} = 2.1 Hz, pyC^{3}H), 114.2 (s, pyC$^{3'}$H), 111.7 (s, pyC$^{5'}$H), 53.4 (s, OCH_3), 32.55 (d, J = 26.1 Hz, CH_2), 32.44 (d, J = 24.0 Hz, $P(C(CH_3)_3)_2$), 30.09 (d, J = 13.9 Hz, $P(C(CH_3)_3)_2$). ^{31}P NMR (202 MHz, acetone-d_6, ppm): δ 36.6 (s). Assignments were confirmed by $^{1}H-^{1}H$ COSY, $^{1}H-^{1}H$ TOCSY, $^{1}H-^{13}C$ HSQC, and $^{1}H-^{13}C$ HMBC. HRMS (CSI+) ($C_{20}H_{29}N_2OP$): *m*/*z* calcd, 345.2096 $[M + H]^+$; found, 345.2077 $[M + H]^+$.

Ligand L^H. This synthesis is a modified literature procedure.[28] L^{Me} (1.055 g, 3.065 mmol) was dissolved in 33% HBr in glacial acetic acid (25 mL) and stirred at reflux overnight, with the reflux cooler connected to a gas trap filled with NaOH (1 M). The solution was cooled to room temperature and neutralized with 25 mL of a 21.6 M NaOH solution. The mixture was extracted with dichloromethane (3 × 20 mL), and the combined organic layers were dried over Na_2SO_4 and evaporated in vacuo to yield the product as a light yellow powder (1.012 g, 69%). ^{1}H NMR (500 MHz, CD_2Cl_2, ppm): δ 11.97 (s, 1H, OH), 7.72 (t, J_{HH} = 7.8 Hz, 1H, pyH^4), 7.64 (d, J_{HH} = 7.8 Hz, 1H, pyH^3), 7.56 (dd, J_{HH} = 9.1, 7.0 Hz, 1H, py$H^{4'}$), 7.52, (d, J_{HH} = 7.8 Hz, 1H, pyH^5), 6.93 (d, J_{HH} = 7.0 Hz, 1H, py$H^{3'}$), 6.63 (d, J_{HH} = 9.0 Hz, 1H, py$H^{5'}$), 3.16 (d, J_{PH} = 3.2 Hz, 2H, CH_2), 1.16 (d, J_{PH} = 11.1 Hz, 18H, $P(C(CH_3)_3)_2$). ^{13}C NMR (75 MHz, CD_2Cl_2, ppm): δ 163.8 (s, pyC), 163.2 (d, J_{PC} = 15.0 Hz, pyC^6), 147.0 (s, pyC), 142.9 (s, pyC), 141.7 (s, pyC$^{4'}$H), 137.7 (s, pyC^{4}H), 125.5 (d, J_{PC} = 9.5 Hz, pyC^{5}H), 121.3 (s, pyC$^{5'}$H), 117.1 (d, J_{PC} = 1.5 Hz, pyC^{3}H), 103.9 (s, 1C, pyC$^{3'}$H), 32.3 (d, J_{PC} = 22.5 Hz, $P(C(CH_3)_3)_2$), 31.8 (d, J_{PC} = 25.3 Hz, CH_2), 29.8 (d, J_{PC} = 13.6 Hz, $P(C(CH_3)_3)_2$). Assignments were confirmed by $^{1}H-^{1}H$ COSY, $^{1}H-^{13}C$ HSQC, and ^{13}C APT. ^{31}P NMR (202 MHz, CD_2Cl_2, ppm): δ 37.5 (s). HR-MS (CSI+) ($C_{19}H_{27}N_2OP$): *m*/*z* calcd, 331.1939 $[M + H]^+$; found, 331.1943 $[M + H]^+$.

Complex 1, Ru(Cl)(CO)(H)(L^H*).* $RuCl(CO)(H)(PPh_3)_3$ (342.7 mg, 0.36 mmol) and L^H (118.8 mg, 0.36 mmol) were dissolved in 10 mL of THF. The solution was heated to 50 °C and stirred overnight. The reddish orange suspension was cooled to room temperature and filtered. The solid was washed with cold Et_2O (3 × 5 mL), and the product was obtained as an orange solid (120.1 mg, 67%). ^{1}H NMR (500 MHz, CD_3OD, ppm): δ 8.18 (d, J_{HH} = 8.0 Hz, 1H, pyH^3), 8.02 (t, J_{HH} = 7.9 Hz, 1H, pyH^4), 7.88 (t, J_{HH} = 7.9 Hz, 1H, py$H^{4'}$), 7.80 (d, J_{HH} = 8.0 Hz, 1H, py$H^{3'}$), 7.76 (d, J_{HH} = 7.8 Hz, 1H, pyH^5), 7.04 (d, J_{HH} = 8.4 Hz, 1H, py$H^{5'}$), 3.98−3.60 (ABX system, centered around 3.90 and 3.68 ppm, J_{HH} = 17.4 Hz, J_{PH_A} = 11.2 Hz, J_{PH_B} = 7.4 Hz, 2H, CH_AH_B), 1.43 (d, J_{PH} = 13.5 Hz, 9H, $PC(CH_{A3})_3$), 1.20 (d, J_{PH} = 13.4 Hz, 9H, $PC(CH_{B3})_3$), −19.32 (br d, J_{PH} = 23.8 Hz, 1H, Ru*H*). py-OH was not observed, and the Ru-H signal was weak and broadened due to H−D exchange with CD_3OD. ^{13}C NMR (126 MHz, CD_3OD, ppm): δ 208.1 (d, J = 16.5 Hz, Ru-CO), 167.0 (s, pyC) 164.2 (d, J_{PC} = 4.6 Hz, pyC^6), 158.3 (s, pyC), 156.6 (s, pyC), 141.5 (s, pyC$^{4'}$H), 140.1 (s, pyC^{4}H), 124.8 (d, J_{PC} = 8.9 Hz, pyC^{5}H), 121.0 (s, pyC^{3}H), 115.0 (s, pyC$^{3'}$H), 114.3 (s, pyC$^{5'}$H), 37.67 (d, J_{PC} = 25.4 Hz, CH_2P), 37.63 (d, J_{PC} = 17.2 Hz, $PC_A(CH_3)_3$), 37.59 (d, J_{PC} = 16.9 Hz, $PC_B(CH_3)_3$), 29.6 (d, J_{PC} = 4.2 Hz, $PC(C_AH_3)_3$), 28.8 (d, J = 3.4 Hz, $PC(C_BH_3)_3$). Assignments were confirmed by $^{1}H-^{1}H$ COSY and $^{1}H-^{13}C$ HSQC. ^{31}P NMR (202 MHz, CD_3OD, ppm): δ 104.4 (s). IR (ATR, cm^{-1}): 1995 (m), 1916 (s), 1598 (m), 1566 (m). HR-MS (CSI^+) ($C_{20}H_{28}ClN_2O_2PRu$): *m*/*z* calcd, 461.0937 $[M - Cl]^+$; found, 461.0936 $[M - Cl]^+$.

Complex 1^{Me}*, Ru(Cl)(CO)(H)(*L^{Me}*).* This complex was synthesized in the same manner as complex **1**, but from L^{Me} (115.2 mg, 0.334 mmol) and $RuCl(CO)(H)(PPh_3)_3$ (318.2 mg, 0.334 mmol), and was obtained as an orange-red powder (155.0 mg, 91%). ^{1}H NMR (400 MHz, acetonitrile-d_3, ppm): δ 8.17 (d, J = 8.1 Hz, 1H), 8.12 (t, J = 8.1

DOI: 10.1021/acs.organomet.7b00111
Organometallics 2017, 36, 1541−1549

Hz, 1H), 8.04 (t, J = 8.1 Hz, 1H), 7.94 (d, J = 7.8 Hz, 1H), 7.63 (d, J = 7.6 Hz, 1H), 7.25 (d, J = 8.6 Hz, 1H), 4.16 (s, 3H), 3.87 (dd, J = 17.4, 11.3 Hz, 1H), 3.73 (dd, J = 17.3, 7.9 Hz, 1H), 1.42 (d, J = 13.7 Hz, 9H), 1.22 (d, J = 13.7 Hz, 9H), −14.93 (d, J = 24.3 Hz, 1H). ^{31}P NMR (162 MHz, acetonitrile-d_3, ppm): δ 105.9 (s). ^{13}C NMR (126 MHz, CD_2Cl_2, ppm): δ 208.71 (d, J = 15.5 Hz), 164.83 (s), 161.75 (s), 155.52 (d, J = 32.3 Hz), 139.51 (s), 136.98 (s), 128.84 (s), 122.64 (d, J = 9.0 Hz), 119.68 (s), 115.21 (s), 107.53 (s), 56.81 (s), 37.53−37.13 (m), 36.33 (d, J = 24.7 Hz), 29.79 (d, J = 4.3 Hz), 28.74 (d, J = 3.4 Hz). HR-MS (CSI$^+$) ($C_{21}H_{30}ClN_2O_2PRu$): m/z calcd, 510.07769, 475.10884 [M − Cl]; found, 475.11294 [M − Cl]. IR (ATR, cm^{-1}): 2000 (m), 1901 (s), 1596 (m), 1569 (m).

Complex 1′, Ru(CO)(H)(L). In the glovebox, complex **1** (16.1 mg, 32.5 μmol) and NaOMe (1.9 mg, 35.1 μmol, 1.1 equiv) were mixed in 1.0 mL of CD_3OD and stirred for 30 min. The red solution was filtered into an NMR tube and investigated using NMR spectroscopy. ^{1}H NMR (300 MHz, CD_3OD, ppm): δ 7.97 (d, J_{HH} = 8.1 Hz, 1H, py*H*), 7.90 (t, J_{HH} = 7.8 Hz, 1H, py*H*), 7.62 (d, J_{HH} = 7.5 Hz, 1H, py*H*), 7.47 (dd, J_{HH} = 8.5, 7.2 Hz, 1H, py*H*), 7.22 (d, J_{HH} = 7.3 Hz, 1H, py*H*), 6.62 (d, J_{HH} = 8.4 Hz, 1H, py*H*), 3.90−3.55 (ABX system, centered around 3.80 and 3.63 ppm, J_{HH} = 17.3 Hz, J_{PH_A} = 10.9 Hz, J_{PH_B} = 7.3 Hz, 2H, CH_2), 1.41 (d, J_{PH} = 13.3 Hz, 9H, PC(CH_{A3})$_3$), 1.19 (d, J_{PH} = 13.1 Hz, 9H, PC(CH_{B3})$_3$), −19.47 (d, J_{PH} = 25.0 Hz, 1H, Ru*H*). ^{31}P NMR (121 MHz, CD_3OD, ppm): δ 102.7 (s). ^{13}C NMR was broadened to such an extent that not all signals could be identified even after prolonged measurement.

General Procedure for Formic Acid Dehydrogenation Experiments. In a Schlenk flask equipped with a condenser and containing a magnetic stirrer were placed 10 mol % of complex **1** and 10 mol % of KO^{t}Bu in 1 mL of dioxane. The reaction mixture was heated to 75 °C and stirred for 10 min. Formic acid was added (10 μL), and the evolved gas was collected volumetrically using a buret and converted to molar equivalents using the van der Waals equation of state (eqs 1 and 2 for H_2 and CO_2, respectively):

$$V_{H_2} = \frac{RT}{p} + b - \frac{a}{RT} = 24.49\ \text{L/mol} \quad (1)$$

where R = 8.3145 m^3 Pa mol^{-1} K^{-1}, T = 298.15 K, p = 101325 Pa, b = 26.7 × 10^{-6} m^3 mol^{-1}, and a = 2.49 × 10^{-10} Pa m^3 mol^{-2}and

$$V_{CO_2} = \frac{RT}{p} + b - \frac{a}{RT} = 24.42\ \text{L/mol} \quad (2)$$

where a = 36.5 × 10^{-10} Pa m^3 mol^{-2} and b = 42.7 × 10^{-6} m^3 mol^{-1}. Evolved gases were analyzed with a G·A·S Compact GC instrument (Rt-MSieve 5A 20 m × 0.32 mm + Rt-Q-bond 2 m × 0.32 mm)

General Procedure for Catalytic Alcohol Dehydrogenative Esterification. In a Schlenk flask containing a magnetic stirrer, 1 mol % of catalyst, and 1 mol % of base were added the distilled alcohol (1 mmol) as substrate, 10 μL p-xylene as an internal standard, and 2 mL of toluene. The mixture was stirred at 117 °C in an open system, unless stated otherwise. Aliquots were taken from the mixture during the reaction, which were subsequently filtered over a plug of silica and analyzed by GC and ^{1}H NMR spectroscopy.

X-ray Crystallography. X-ray intensities were measured on a Bruker D8 Quest Eco diffractometer equipped with a Triumph monochromator (λ = 0.71073 Å) and a CMOS Photon 50 detector at a temperature of 150(2) K. Intensity data were integrated with the Bruker APEX2 software.[29] Absorption correction and scaling was performed with SADABS.[30] The structures were solved with the program SHELXL.[29] Least-squares refinement was performed with SHELXL-2013[31] against F^2 of all reflections. Non-hydrogen atoms were refined with anisotropic displacement parameters. The H atoms were placed at calculated positions using the instruction AFIX 13, AFIX 43, or AFIX 137 with isotropic displacement parameters having values 1.2 or 1.5 times the U_{eq} value of the attached C atoms. The O−H hydrogen atom was refined freely with isotropic displacement parameters. Details for complex $\mathbf{1}_{\mathbf{MeCN}}$, [Ru(CO)(H)(L^H)(NCMe)]-Cl: $C_{22}H_{31}ClN_3O_2PRu$, fw = 536.99, yellow block, 0.385 × 0.184 × 0.119 mm, monoclinic $P2_1/n$ (No. 14)), a = 10.0476(3) Å, b = 13.0268(4) Å, c = 18.8205(6) Å, β = 95.685(2)°, V = 2451.26(13) Å^3, Z = 4, D_x = 1.455 g/cm^3, μ = 0.836 mm^{-1}. A total of 92544 reflections were measured up to a resolution of $(\sin\theta/\lambda)_{max}$ = 0.74 Å^{-1}, with 6151 unique reflections (R_{int} = 0.1050), of which 4768 were observed ($I > 2\sigma(I)$); 285 parameters were refined with 0 restraints. R1/wR2 ($I > 2\sigma(I)$): 0.0315/0.0610. R1/wR2 (all reflections): 0.0546/0.0689. S = 1.023. The residual electron density was between −0.55 and 0.62 e/Å^3. CCDC 1530189.

Computational Details. Geometry optimizations were carried out with the Turbomole program package,[32] coupled to the PQS Baker optimizer[33] via the BOpt package.[34] We used the BP86,[35,36] TPSS,[37,38] or B3-LYP[35,36,39] functional in combination with the def2-TZVP basis set.[40,41] Grimme's dispersion corrections (version 3, disp3) were used to include van der Waals interactions.[42] All minima (no imaginary frequencies) and transition states (one imaginary frequency) were characterized by calculating the Hessian matrix. ZPE and gas-phase thermal corrections (273 K) were calculated from these analyses.

■ ASSOCIATED CONTENT

Supporting Information

The Supporting Information is available free of charge on the ACS Publications website at DOI: 10.1021/acs.organomet.7b00111.

NMR spectra of new compounds, computational data, and crystallographic details (PDF)
Computational data (XYZ)
Crystallographic data (CIF)

■ AUTHOR INFORMATION

Corresponding Author

*E-mail for J.I.v.d.V.: j.i.vandervlugt@uva.nl.

ORCID

Jarl Ivar van der Vlugt: 0000-0003-0665-9239

Notes

The authors declare no competing financial interest.

■ ACKNOWLEDGMENTS

This research was funded by the National Research School Combination on Catalysis (NRSC-C). We thank Ed Zuidinga for MS analysis, Prof. Dr. Bas de Bruin for access to the computational facilities, and Dr. Maxime A. Siegler (John Hopkins University) for tips and tricks regarding X-ray crystallography.

■ REFERENCES

(1) (a) Khusnutdinova, J. R.; Milstein, D. *Angew. Chem., Int. Ed.* **2015**, *54*, 12236−12273. (b) Li, H.; Zheng, B.; Huang, K.-W. *Coord. Chem. Rev.* **2015**, *293*−*294*, 116−138.

(2) (a) Kuwata, S.; Ikariya, T. *Chem. Commun.* **2014**, *50*, 14290−14300. (b) McSkimming, A.; Bhadbhade, M. M.; Colbran, S. B. *Angew. Chem., Int. Ed.* **2013**, *52*, 3411−3416. (c) Harman, W. H.; Peters, J. C. *J. Am. Chem. Soc.* **2012**, *134*, 5080−5082. (d) Kuwata, S.; Ikariya, T. *Chem. - Eur. J.* **2011**, *17*, 3542−3556. (e) Gunanathan, C.; Gnanaprakasam, B.; Iron, M. A.; Shimon, L. J. W.; Milstein, D. *J. Am. Chem. Soc.* **2010**, *132*, 14763−14765. (f) Kuwata, S.; Ikariya, T. *Dalton Trans.* **2010**, *39*, 2984−2992.

(3) Younus, H. A.; Ahmad, N.; Su, W.; Verpoort, F. *Coord. Chem. Rev.* **2014**, *276*, 112−152.

(4) (a) van der Vlugt, J. I.; Reek, J. N. H. *Angew. Chem., Int. Ed.* **2009**, *48*, 8832−8846. (b) Benito-Garagorri, D.; Kirchner, K. *Acc. Chem. Res.* **2008**, *41*, 201−213. (c) Gunanathan, C.; Milstein, D. *Chem. Rev.* **2014**, *114*, 12024−12087. For bipyridine-phosphine derivatives, see: (d) Balaraman, E.; Gnanaprakasam, B.; Shimon, L. J. W.; Milstein, D. *J. Am. Chem. Soc.* **2010**, *132*, 16756−16758. (e) Balaraman, E.; Gunanathan, C.; Zhang, J.; Shimon, L. J. W.; Milstein, D. *Nat. Chem.*

DOI: 10.1021/acs.organomet.7b00111
Organometallics 2017, 36, 1541−1549

2011, *3*, 609−614. (f) Balaraman, E.; BenDavid, Y.; Milstein, D. *Angew. Chem., Int. Ed.* **2011**, *50*, 11702−11705. (g) Balaraman, E.; Fogler, E.; Milstein, D. *Chem. Commun.* **2012**, *48*, 1111−1113. See also: (h) Gloaguen, Y.; Rebreyend, C.; Lutz, M.; Kumar, P.; Huber, M.; van der Vlugt, J. I.; Schneider, S.; de Bruin, B. *Angew. Chem., Int. Ed.* **2014**, *53*, 6814−6818.

(5) (a) Umehara, K.; Kuwata, S.; Ikariya, T. *J. Am. Chem. Soc.* **2013**, *135*, 6754−6757. (b) Toda, T.; Kuwata, S.; Ikariya, T. *Chem. - Eur. J.* **2014**, *20*, 9539−9542. (c) Toda, T.; Yoshinari, A.; Ikariya, T.; Kuwata, S. *Chem. - Eur. J.* **2016**, *22*, 16675−16683. (d) Jozak, T.; Zabel, D.; Schubert, A.; Sun, Y.; Thiel, W. R. *Eur. J. Inorg. Chem.* **2010**, *2010*, 5135−5145. (e) Wang, L.; Yang, Q.; Chen, H.; Li, R. *Inorg. Chem. Commun.* **2011**, *14*, 1884−1888.

(6) (a) Geri, J. B.; Szymczak, N. K. *J. Am. Chem. Soc.* **2015**, *137*, 12808−12814. (b) Moore, C. M.; Bark, B.; Szymczak, N. K. *ACS Catal.* **2016**, *6*, 1981−1990. (c) Wang, W.-H.; Muckerman, J. T.; Fujita, E.; Himeda, Y. *New J. Chem.* **2013**, *37*, 1860−1866. (d) Moore, C. M.; Szymczak, N. K. *Chem. Commun.* **2013**, *49*, 400−402. (e) Kawahara, R.; Fujita, K.-i.; Yamaguchi, R. *Angew. Chem., Int. Ed.* **2012**, *51*, 12790−12794. (f) Wang, W.; Muckerman, J. T.; Fujita, E.; Himeda, Y. *ACS Catal.* **2013**, *3*, 856−860. (g) Wang, W.; Hull, J. F.; Muckerman, J. T.; Fujita, E.; Himeda, Y. *Energy Environ. Sci.* **2012**, *5*, 7923−7926.

(7) Reviews: (a) Ikariya, T.; Murata, K.; Noyori, R. *Org. Biomol. Chem.* **2006**, *4*, 393−406. (b) Noyori, R.; Hashiguchi, S. *Acc. Chem. Res.* **1997**, *30*, 97−102. (c) Zweifel, T.; Naubron, J.-V.; Grützmacher, H. *Angew. Chem., Int. Ed.* **2009**, *48*, 559−563. (d) Schneider, S.; Meiners, J.; Askevold, B. *Eur. J. Inorg. Chem.* **2012**, *2012*, 412−429. (e) Zhao, B.; Han, Z.; Ding, K. *Angew. Chem., Int. Ed.* **2013**, *52*, 4744−4788. (f) Morris, R. H. *Acc. Chem. Res.* **2015**, *48*, 1494−1502.

(8) Recent examples: (a) Nielsen, M.; Kammer, A.; Cozzula, D.; Junge, H.; Gladiali, S.; Beller, M. *Angew. Chem., Int. Ed.* **2011**, *50*, 9593−9597. (b) Bertoli, M.; Choualeb, A.; Lough, A. J.; Moore, B.; Spasyuk, D.; Gusev, D. G. *Organometallics* **2011**, *30*, 3479−3482. (c) Nielsen, M.; Alberico, E.; Baumann, W.; Drexler, H.-J.; Junge, H.; Gladiali, S.; Beller, M. *Nature* **2013**, *495*, 85−89. (d) Zuo, W.; Lough, A. J.; Li, Y. F.; Morris, R. H. *Science* **2013**, *342*, 1080−1083. (e) Chakraborty, S.; Lagaditis, P. O.; Förster, M.; Bielinski, E. A.; Hazari, N.; Holthausen, M. C.; Jones, W. D.; Schneider, S. *ACS Catal.* **2014**, *4*, 3994−4003. (f) Chakraborty, S.; Brennessel, W. W.; Jones, W. D. *J. Am. Chem. Soc.* **2014**, *136*, 8564−8567. (g) Bonitatibus, P. J., Jr.; Chakraborty, S.; Doherty, M. D.; Siclovana, O.; Jones, W. D.; Soloveichik, G. L. *Proc. Natl. Acad. Sci. U. S. A.* **2015**, *112*, 1687−1692. (h) Alberico, E.; Lennox, A. J. J.; Vogt, L. K.; Jiao, H.; Baumann, W.; Drexler, H.-J.; Nielsen, M.; Spannenberg, A.; Checinski, M. P.; Junge, H.; Beller, M. *J. Am. Chem. Soc.* **2016**, *138*, 14890−14904. (i) Prokopchuk, D. E.; Lough, A. J.; Rodriguez-Lugo, R. E.; Morris, R. H.; Grützmacher, H. *Chem. Commun.* **2016**, *52*, 6138−6141.

(9) Work from our group: (a) Gloaguen, Y.; Jongens, L. M.; Lutz, M.; Reek, J. N. H.; de Bruin, B.; van der Vlugt, J. I. *Organometallics* **2013**, *32*, 4284−4291. (b) Jongbloed, L. S.; de Bruin, B.; Reek, J. N. H.; Lutz, M.; van der Vlugt, J. I. *Chem. - Eur. J.* **2015**, *21*, 7297−7305. (c) Jongbloed, L. S.; García-López, D.; van Heck, R.; Siegler, M. A.; Carbó, J. J.; van der Vlugt, J. I. *Inorg. Chem.* **2016**, *55*, 8041−8047. Contributions from other groups: (d) Ghatak, K.; Mane, M.; Vanka, K. *ACS Catal.* **2013**, *3*, 920−927. (e) Taghizadeh Ghoochany, L.; Kerner, C.; Farsadpour, S.; Menges, F.; Sun, Y.; Niedner-Schatteburg, G.; Thiel, W. R. *Eur. J. Inorg. Chem.* **2013**, *2013*, 4305−4317. (f) Gutsulyak, D. V.; Piers, W. E.; Borau-Garcia, J.; Parvez, M. *J. Am. Chem. Soc.* **2013**, *135*, 11776−11779. (g) Boulho, C.; Djukic, J.-P. *Dalton Trans.* **2010**, *39*, 8893−8905. (h) Stolzenberg, A. M.; Muetterties, E. L. *Organometallics* **1985**, *4*, 1739−1742.

(10) (a) Tang, Z.; Otten, E.; Reek, J. N. H.; van der Vlugt, J. I.; de Bruin, B. *Chem. - Eur. J.* **2015**, *21*, 12683−12693. (b) Tang, Z.; Mandal, S.; Paul, N. D.; Lutz, M.; Li, P.; van der Vlugt, J. I.; de Bruin, B. *Org. Chem. Front.* **2015**, *2*, 1561−1577.

(11) (a) Fogler, E.; Garg, J. A.; Hu, P.; Leitus, G.; Shimon, L. J. W.; Milstein, D. *Chem. - Eur. J.* **2014**, *20*, 15727−15731. (b) Langer, R.; Fuchs, I.; Vogt, M.; Balaraman, E.; Diskin-Posner, Y.; Shimon, L. J. W.; Ben-David, Y.; Milstein, D. *Chem. - Eur. J.* **2013**, *19*, 3407−3414.

(12) (a) Balaraman, E.; Khaskin, E.; Leitus, G.; Milstein, D. *Nat. Chem.* **2013**, *5*, 122−125. (b) Khaskin, E.; Iron, M. A.; Shimon, L. J. W.; Zhang, J.; Milstein, D. *J. Am. Chem. Soc.* **2010**, *132*, 8542−8543. (c) Gunanathan, C.; Ben-David, Y.; Milstein, D. *Science* **2007**, *317*, 790−792. (d) Zhang, J.; Leitus, G.; Ben-David, Y.; Milstein, D. *J. Am. Chem. Soc.* **2005**, *127*, 10840−10841. (e) Zhang, J.; Gandelman, M.; Shimon, L. J. W.; Rozenberg, H.; Milstein, D. *Organometallics* **2004**, *23*, 4026−4033.

(13) (a) van der Vlugt, J. I.; Pidko, E. A.; Vogt, D.; Lutz, M.; Spek, A. L. *Inorg. Chem.* **2009**, *48*, 7513−7515. (b) van der Vlugt, J. I.; Lutz, M.; Pidko, E. A.; Vogt, D.; Spek, A. L. *Dalton Trans.* **2009**, 1016−1023. (c) van der Vlugt, J. I.; Siegler, M. A.; Janssen, M.; Vogt, D.; Spek, A. L. *Organometallics* **2009**, *28*, 7025−7032. (d) Bauer, R. C.; Gloaguen, Y.; Lutz, M.; Reek, J. N. H.; de Bruin, B.; van der Vlugt, J. I. *Dalton Trans.* **2011**, *40*, 8822−8829. (e) van der Vlugt, J. I.; Pidko, E. A.; Bauer, R. C.; Gloaguen, Y.; Rong, M. K.; Lutz, M. *Chem. - Eur. J.* **2011**, *17*, 3850−3854. (f) de Boer, S. Y.; Gloaguen, Y.; Reek, J. N. H.; Lutz, M.; van der Vlugt, J. I. *Dalton Trans.* **2012**, *41*, 11276−11283. (g) de Boer, S. Y.; Gloaguen, Y.; Lutz, M.; van der Vlugt, J. I. *Inorg. Chim. Acta* **2012**, *380*, 336−342. (h) Gloaguen, Y.; Jacobs, W.; de Bruin, B.; Lutz, M.; van der Vlugt, J. I. *Inorg. Chem.* **2013**, *52*, 1682−1684. (i) Broere, D. L. J.; de Bruin, B.; Reek, J. N. H.; Lutz, M.; Dechert, S.; van der Vlugt, J. I. *J. Am. Chem. Soc.* **2014**, *136*, 11574−11577. (j) Vreeken, V.; Siegler, M. A.; de Bruin, B.; Reek, J. N. H.; Lutz, M.; van der Vlugt, J. I. *Angew. Chem., Int. Ed.* **2015**, *54*, 7055−7059. (k) Oldenhof, S.; Terrade, F. G.; Lutz, M.; van der Vlugt, J. I.; Reek, J. N. H. *Organometallics* **2015**, *34*, 3209−3215. (l) Oldenhof, S.; Lutz, M.; van der Vlugt, J. I.; Reek, J. N. H. *Chem. Commun.* **2015**, *51*, 15200−15203. (m) Broere, D. L. J.; Metz, L. L.; de Bruin, B.; Reek, J. N. H.; Siegler, M. A.; van der Vlugt, J. I. *Angew. Chem., Int. Ed.* **2015**, *54*, 1516−1520. (n) Broere, D. L. J.; Modder, D. K.; Blokker, E.; Siegler, M. A.; van der Vlugt, J. I. *Angew. Chem., Int. Ed.* **2016**, *55*, 2406−2410. (o) Vreeken, V.; Siegler, M. A.; van der Vlugt, J. I. *Chem. - Eur. J.* **2017**, DOI: 10.1002/chem.201700360.

(14) Hoang, T. N. Y.; Humbert-Droz, M.; Dutronc, T.; Guénée, L.; Besnard, C.; Piguet, C. *Inorg. Chem.* **2013**, *52*, 5570−5580.

(15) Ripin, D. H.; Evans, D. A. *pKa's of Inorganic and Oxo-Acids.* http://evans.harvard.edu/pdf/evans_pKa_table.pdf (accessed Oct 8, 2015).

(16) We have not investigated deprotonation at lower *T*, but the reaction with weaker bases such as DBU suggests that the −OH group is more acidic than the $-CH_2$ linker, excluding intramolecular proton transfer via initial reactivity at the methylene spacer. This is in contrast to observations on our 2-phosphinomethyl-6-phenylpyridine ligand described in ref 9b.

(17) Recent reviews: (a) Eppinger, J.; Huang, K.-W. *ACS Energy Lett.* **2017**, *2*, 188−195. (b) Mellmann, D.; Sponholz, P.; Junge, H.; Beller, M. *Chem. Soc. Rev.* **2016**, *45*, 3954−3988. (c) Singh, A. K.; Singh, S.; Kumar, A. *Catal. Sci. Technol.* **2016**, *6*, 12−40. (d) Laurenczy, G.; Dyson, P. J. *J. Braz. Chem. Soc.* **2014**, *25*, 2157−2163. (e) Grasemann, M.; Laurenczy, G. *Energy Environ. Sci.* **2012**, *5*, 8171−8181.

(18) (a) Gao, Y.; Kuncheria, J.; Puddephatt, R. J.; Yap, G. P. A. *Chem. Commun.* **1998**, 2365−2366. (b) Loges, B.; Boddien, A.; Junge, H.; Beller, M. *Angew. Chem., Int. Ed.* **2008**, *47*, 3962−3965. (c) Fellay, C.; Dyson, P. J.; Laurenczy, G. *Angew. Chem., Int. Ed.* **2008**, *47*, 3966−3968. (d) Boddien, A.; Loges, B.; Junge, H.; Beller, M. *ChemSusChem* **2008**, *1*, 751−758. (e) Boddien, A.; Loges, B.; Junge, H.; Gärtner, F.; Noyes, J. R.; Bellera, M. *Adv. Synth. Catal.* **2009**, *351*, 2517−2520. (f) Filonenko, G. A.; Conley, M. P.; Copéret, C.; Lutz, M.; Hensen, E. J. M.; Pidko, E. A. *ACS Catal.* **2013**, *3*, 2522−2526. (g) Mellone, I.; Peruzzini, M.; Rosi, L.; Mellmann, D.; Junge, H.; Beller, M.; Gonsalvi, L. *Dalton Trans.* **2013**, *42*, 2495−2501. (h) Filonenko, G. A.; van Putten, R.; Schulpen, E. N.; Hensen, E. J. M.; Pidko, E. A. *ChemCatChem* **2014**, *6*, 1526−1530. (i) Thevenon, A.; Frost-Pennington, E.; Weijia, G.; Dalebrook, A. F.; Laurenczy, G. *ChemCatChem* **2014**, *6*, 3146−3152. (j) Czaun, M.; Goeppert, A.; Kothandaraman, J.; May, R. B.; Haiges, R.; Prakash, G. K. S.; Olah, G.

DOI: 10.1021/acs.organomet.7b00111
Organometallics 2017, 36, 1541−1549

A. *ACS Catal.* **2014**, *4*, 311−320. (k) Guerriero, A.; Bricout, H.; Sordakis, K.; Peruzzini, M.; Monflier, E.; Hapiot, F.; Laurenczy, G.; Gonsalvi, L. *ACS Catal.* **2014**, *4*, 3002−3012. (l) Pan, Y.; Pan, C. L.; Zhang, Y.; Li, H.; Min, S.; Guo, X.; Zheng, B.; Chen, H.; Anders, A.; Lai, Z.; Zheng, J.; Huang, K.-W. *Chem. - Asian J.* **2016**, *11*, 1357−1360. (m) Guan, C.; Zhang, D.-D.; Pan, Y.; Iguchi, M.; Ajitha, M. J.; Hu, J.; Li, H.; Yao, C.; Huang, M.-H.; Min, S.; Zheng, J.; Himeda, Y.; Kawanami, H.; Huang, K.-W. *Inorg. Chem.* **2017**, *56*, 438−445.

(19) Systems that work under base-free conditions: (a) Hull, J. F.; Himeda, Y.; Wang, W. H.; Hashiguchi, B.; Periana, R.; Szalda, D. J.; Muckerman, J. T.; Fujita, E. *Nat. Chem.* **2012**, *4*, 383−388. (b) Oldenhof, S.; de Bruin, B.; Lutz, M.; Siegler, M. A.; Patureau, F. W.; van der Vlugt, J. I.; Reek, J. N. H. *Chem. - Eur. J.* **2013**, *19*, 11507−11511. (c) Rodríguez-Lugo, R. E.; Trincado, M.; Vogt, M.; Tewes, F.; Santiso-Quinones, G.; Grützmacher, H. *Nat. Chem.* **2013**, *5*, 342−347. (d) Oldenhof, S.; Lutz, M.; de Bruin, B.; van der Vlugt, J. I.; Reek, J. N. H. *Chem. Sci.* **2015**, *6*, 1027−1034. (e) Oldenhof, S.; van der Vlugt, J. I.; Reek, J. N. H. *Catal. Sci. Technol.* **2016**, *6*, 404−408. (f) Jongbloed, L. S.; de Bruin, B.; Reek, J. N. H.; Lutz, M.; van der Vlugt, J. I. *Catal. Sci. Technol.* **2016**, *6*, 1320−1327.

(20) Formic acid dehydrogenation with the bipyridine-methylphosphine Ru(PNN) system: Hu, P.; Diskin-Posner, Y.; Ben-David, Y.; Milstein, D. *ACS Catal.* **2014**, *4*, 2649−2652.

(21) Montag, M.; Zhang, J.; Milstein, D. *J. Am. Chem. Soc.* **2012**, *134*, 10325−10328.

(22) See reference 12d. For catalytic applications of the bipyridine-methylphosphine PNN derivative in the cross-dehydrogenative coupling reaction of primary and secondary alcohols, see: (a) Srimani, D.; Balaraman, E.; Gnanaprakasam, B.; Ben-David, Y.; Milstein, D. *Adv. Synth. Catal.* **2012**, *354*, 2403−2406. These reactions also typically require 24 h for ±95% conversion. For related work, see: (b) Srimani, D.; Balaraman, E.; Hu, P.; Ben-David, Y.; Milstein, D. *Adv. Synth. Catal.* **2013**, *355*, 2525−2530. (c) Srimani, D.; Ben-David, Y.; Milstein, D. *Angew. Chem., Int. Ed.* **2013**, *52*, 4012−4015. For the reverse reaction, i.e. decomposition of polymeric esters into monomers using the bipyridine-methylphosphine Ru(PNN) system, see: (d) Krall, E. M.; Klein, T. W.; Andersen, R. J.; Nett, A. J.; Glasgow, R. W.; Reader, D. S.; Dauphinais, B. C.; Mc Ilrath, S. P.; Fischer, A. A.; Carney, M. J.; Hudson, D. J.; Robertson, N. J. *Chem. Commun.* **2014**, *50*, 4884−4887.

(23) If deprotonation in toluene does occur, a strong ion pairing interaction between **1′** and the protonated DBU could be another explanation for the lack of reactivity.

(24) Li, H.; Wang, X.; Huang, F.; Lu, G.; Jiang, J.; Wang, Z.-X. *Organometallics* **2011**, *30*, 5233−5247.

(25) For related recent work implying proton-shuttling mechanisms, see: (a) Chen, T.; Li, H.; Qu, S.; Zheng, B.; He, L.; Lai, Z.; Wang, Z.-X.; Huang, K.-W. *Organometallics* **2014**, *33*, 4152−4155. (b) Qu, S.; Dang, Y.; Song, C.; Wen, M.; Huang, K.-W.; Wang, Z.-X. *J. Am. Chem. Soc.* **2014**, *136*, 4974−4991. (c) Chakraborty, S.; Lagaditis, P. O.; Förster, M.; Bielinski, E. A.; Hazari, N.; Holthausen, M. C.; Jones, W. D.; Schneider, S. *ACS Catal.* **2014**, *4*, 3994−4003. For computational work involving proton shuttling related to Ru(PNN) systems, see: (d) Li, H.; Hall, M. B. J. *J. Am. Chem. Soc.* **2014**, *136*, 383−395. (e) Hasanayn, F.; Al-Assi, L. M.; Moussawi, R. N.; Srour Omar, B. *Inorg. Chem.* **2016**, *55*, 7886−7902.

(26) Fulmer, G. R.; Miller, A. J. M.; Sherden, N. H.; Gottlieb, H. E.; Nudelman, A.; Stoltz, B. M.; Bercaw, J. E.; Goldberg, K. I. *Organometallics* **2010**, *29*, 2176−2179.

(27) Farr, J. P.; Olmstead, M. M.; Balch, A. L. *J. Am. Chem. Soc.* **1980**, *102*, 6654−6656.

(28) Knebel, W. J.; Angelici, R. J. *Inorg. Chim. Acta* **1973**, *7*, 713−716.

(29) *APEX2* software; Bruker, Madison WI, USA, 2014.

(30) Sheldrick, G. M. *SADABS*, Universität Göttingen, Germany, 2008.

(31) Sheldrick, G. M. *SHELXL2013*, University of Göttingen, Germany, 2013.

(32) Ahlrichs, R. *Turbomole Version 6.5*, Theoretical Chemistry Group, University of Karlsruhe.

(33) *PQS version 2.4*; Parallel Quantum Solutions, Fayetteville, Arkansas, USA, 2001. The Baker optimizer is available separately from PQS upon request: Baker, I. *J. Comput. Chem.* **1986**, *7*, 385−395.

(34) Budzelaar, P. H. M. *J. Comput. Chem.* **2007**, *28*, 2226−2236.

(35) Becke, A. D. *Phys. Rev. A: At., Mol., Opt. Phys.* **1988**, *38*, 3098−3100.

(36) Perdew, J. P. *Phys. Rev. B: Condens. Matter Mater. Phys.* **1986**, *33*, 8822−8824.

(37) Perdew, J. P.; Wang, Y. *Phys. Rev. B: Condens. Matter Mater. Phys.* **1992**, *45*, 13244−13249.

(38) Tao, J.; Perdew, J. P.; Staroverov, V. N.; Scuseria, G. E. *Phys. Rev. Lett.* **2003**, *91*, 146401.

(39) Becke, A. D. *J. Chem. Phys.* **1993**, *98*, 1372−1377.

(40) Weigend, F.; Häser, M.; Patzelt, H.; Ahlrichs, R. *Chem. Phys. Lett.* **1998**, *294*, 143−152.

(41) Weigend, F.; Ahlrichs, R. *Phys. Chem. Chem. Phys.* **2005**, *7*, 3297−3305.

(42) Grimme, S.; Antony, J.; Ehrlich, S.; Krieg, H. *J. Chem. Phys.* **2010**, *132*, 154104.

DOI: 10.1021/acs.organomet.7b00111
Organometallics 2017, 36, 1541−1549